J|A|C|S
ARTICLES
Published on Web 06/18/2002

Characterization of the Interface Dipole at Organic/Metal Interfaces

Xavier Crispin,*,†,‡ Victor Geskin,‡ Annica Crispin,† Jérôme Cornil,‡,§ Roberto Lazzaroni,‡,§ William R. Salaneck,† and Jean-Luc Brédas‡,§

Contribution from the Department of Physics and Measurement Technology, Linköping University, S-58183 Linköping, Sweden, Service de Chimie des Matériaux Nouveaux, Centre de Recherche en Electronique et Photonique Moléculaires, Université de Mons-Hainaut, Place du Parc 20, B-7000 Mons, Belgium, and Department of Chemistry, The University of Arizona, Tucson, Arizona 85721-0041

Received January 22, 2002

Abstract: In organics-based (opto)electronic devices, the interface dipoles formed at the organic/metal interfaces play a key role in determining the barrier for charge (hole or electron) injection between the metal electrodes and the active organic layers. The origin of this dipole is rationalized here from the results of a joint experimental and theoretical study based on the interaction between acrylonitrile, a π-conjugated molecule, and transition metal surfaces (Cu, Ni, and Fe). The adsorption of acrylonitrile on these surfaces is investigated experimentally by photoelectron spectroscopies, while quantum mechanical methods based on density functional theory are used to study the systems theoretically. It appears that the interface dipole formed at an organic/metal interface can be divided into two contributions: (i) the first corresponds to the "chemical" dipole induced by a partial charge transfer between the organic layers and the metal upon chemisorption of the organic molecules on the metal surface, and (ii) the second relates to the change in metal surface dipole because of the modification of the metal electron density tail that is induced by the presence of the adsorbed organic molecules. Our analysis shows that the charge injection barrier in devices can be tuned by modulating various parameters: the chemical potential of the bare metal (given by its work function), the metal surface dipole, and the ionization potential and electron affinity of the organic layer.

1. Introduction

In the field of organics-based (opto)electronic devices, increasing attention is being paid to the charge injection process (of holes or electrons) between the metal electrodes and the active organic layers. Metal/π-conjugated material interfaces are present, for instance, in light-emitting diodes, photovoltaic cells, or field-effect transistors; they are thought to be one of the device parameters that most significantly influences the device performance.[1]

Recent experimental data have demonstrated that the efficiency of organic light-emitting diodes (turn-on voltage and luminance) is directly related to the charge injection process between the metal electrodes and the organic materials.[2,3] A traditional simple approach to estimate the hole [electron] injection barrier is to take the difference between the metal work function and the highest occupied molecular orbital, HOMO [lowest unoccupied molecular orbital, LUMO], of the conjugated material, as measured via photoelectron spectroscopy or electrochemistry. However, numerous photoelectron studies and Kelvin probe measurements[4] have demonstrated that the actual situation is more complex, because an interface dipole D_{int} can appear at the conjugated material/metal interface and affect the charge injection barrier.[5−8]

An interface dipole with its negative pole pointing toward the organic layer and its positive pole toward the metal increases the metal work function (i.e., decreases the Fermi energy) and increases the HOMO energy of the organic layer by adding an electrostatic energy; as a result, the hole injection barrier ϕ_{h} is reduced, see Figure 1. Accordingly, reversing the direction of the interface dipole reduces the electron injection barrier ϕ_{e}. Thus, work function increase [decrease] is associated with an improvement of hole [electron] injection. Because the metal

* To whom correspondence should be addressed. E-mail: xavcr@ifm.liu.se.
† Linköping University.
‡ Université de Mons-Hainaut.
§ The University of Arizona.

(1) Salaneck, W. R.; Stafström, S.; Brédas, J. L. *Conjugated Polymer Surfaces and Interfaces: Electronic and Chemical Structure of Interfaces for Polymer Light Emitting Devices*; Cambridge University Press: Cambridge, 1996.
(2) Shen, Y.; Klein, M.; Jacobs, D.; Scott, J. C.; Malliaras, G. *Phys. Rev. Lett.* **2001**, *86*, 3867.
(3) Baldo, M. A.; Forrest, S. R. *Phys. Rev. B* **2001**, *64*, 085201.
(4) Ito, E.; Oji, H.; Hayashi, N.; Ishii, H.; Ouchi, Y.; Seki, K. *Appl. Surf. Sci.* **2001**, *175*, 407.
(5) Ishii, H.; Seki, K. *IEEE Trans. Electron Devices* **1997**, *44*, 1295. Ishii, H.; Sugiyama, K.; Ito, E.; Seki, K. *Adv. Mater.* **1999**, *11*, 605.
(6) Hill, I. G.; Rajagopal, A.; Kahn, A.; Hu, Y. *Appl. Phys. Lett.* **1998**, *73*, 662.
(7) Blochwitz, J.; Fritz, T.; Pfeiffer, M.; Leo, K.; Alloway, D. M.; Lee, P. A.; Armstrong, N. R. *Org. Electron.* **2001**, *2*, 97. Schlettwein, D.; Hesse, K.; Gruhn, N. E.; Lee, P. A.; Nebesny, K. W.; Armstrong, N. R. *J. Phys. Chem. B* **2001**, *105*, 4791.
(8) Nüesch, F.; Rotzinger, F.; Si-Ahmed, L.; Zuppiroli, L. *Chem. Phys. Lett.* **1998**, *288*, 861.

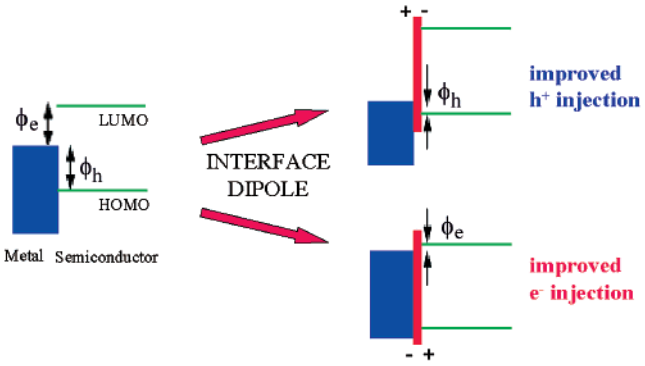

Figure 1. Sketch of the impact of the formation of an interface dipole on the electronic levels at an organic semiconductor/metal interface.

work function is affected, that is, the interface dipole is created, by adsorbing an organic layer, a proposed improvement route for charge injection is to chemisorb molecular species on the metal surface. Indium tin oxide surfaces have, for instance, been modified by protonation or by grafting dipolar molecules.[8,9] With molecules carrying a high dipole moment oriented perpendicular to the metal surface, it has been observed that the total interface dipole can be rather easily tuned by changing chemically the magnitude of the molecular dipole moment.[10−12]

In this work, to illustrate some of the basic issues involved, we focus instead on the origin of the interface dipole created upon adsorption of π-conjugated organic molecules that do not carry a high dipole moment oriented perpendicular to the metal surface; we have taken the example of acrylonitrile (which absorbs flat on transition metal surfaces). The interface dipole has two contributions. The first comes from the change in metal work function because of the perturbation of the metal surface electron density tail related to the presence of the adsorbed (chemisorbed or physisorbed) organic molecules. In addition, when the molecules are actually chemisorbed on the metal surface, their electron density interacts with that of the metal such that new chemical bonds can be formed. Bond formation is accompanied by an electron density flow through the atoms involved in the newly formed bonds, whose direction depends on the relative electronegativities. This partial charge transfer between metal and adsorbate constitutes the second contribution to the interface dipole.

Our results are described in four steps. First, we briefly describe theoretically the geometric structure of acrylonitrile (CH_2═CH−C≡N, AN) chemisorbed on three model metal surfaces: Cu_9(100), Ni_9(100), and Fe_9(100). Second, we show that X-ray photoelectron spectroscopy (XPS) can be exploited to investigate the partial charge transfer between a metal surface and a chemisorbed molecular layer; this is illustrated in the case of AN chemisorbed on Cu, Ni, and Fe polycrystalline surfaces. Third, the phenomenon of partial charge transfer upon chemisorption is theoretically characterized in the framework of density functional theory. Fourth, UV-photoelectron spectroscopy (UPS) is used to determine the metal work function change in the case of (i) chemisorption (illustrated with AN on transition metals), and (ii) physisorption (Xe on various metals, data taken from the literature). Finally, from the results of these investigations, we discuss a route to improve the charge injection process in organics-based (opto)electronic devices via selected adsorption of molecular layers on metal electrodes.

2. Experimental Section

Polycrystalline Ni, Cu, and Fe surfaces were sputtered (ion etched) clean in the ultrahigh vacuum (UHV) preparation chamber of the spectrometer. Neon ions ($P = 4 \times 10^{-7}$ mbar) accelerated under 5 kV are used to clean the metal surfaces at the atomic level. After cleaning, the copper surfaces are free of carbon, nitrogen, and oxygen; the nickel surface exhibits a very low level of contamination from carbon (C(1s) = 283.9 eV) and oxygen (O(1s) = 531.1 eV), while the iron surface does not show any C(1s) signal and only a very weak O(1s) signal at 530.0 eV. Note that, because of the very low levels of contamination, the intensities of the XPS signals corresponding to an adsorbed AN monolayer are much larger than those of the contaminants. The XPS spectra of the adsorbate are not affected by the presence of the small contamination signals.

The AN monolayers were prepared by direct adsorption of gaseous AN molecules on the metal substrate cooled at −90 °C (to increase the sticking coefficient of AN), but kept above the vaporization temperature (so that multilayer formation was inhibited). The gaseous AN molecules were introduced in the chamber with a doser, which provides a higher local pressure around the metal substrate. Once the monolayer was formed, the sample was moved into the analysis chamber of the spectrometer for XPS and UPS measurements. XPS and UPS measurements were done using a Scienta ESCA 200 spectrometer.[13] The ESCA 200 uses monochromatized Al Kα radiation at 1486.6 eV for XPS, or a doubly differentially pumped He-resonance lamp for UPS. The experimental conditions are such that the full width at half-maximum (fwhm) of the gold Au($4f_{7/2}$) line is 0.65 eV. The background pressure in the sample preparation chamber is 3×10^{-10} mbar, and the pressure in the analysis chamber is 1×10^{-10} mbar. Note that all XPS and UPS spectra have been recorded with a takeoff angle of 90°.

3. Theoretical Approach

3.1. Model. To compare the adsorption behavior of acrylonitrile on three different metals (Fe, Ni, Cu), two-layer clusters composed of nine atoms are used to model the (100) surface. Working with flat-surface clusters has several advantages: (i) the geometry of the acrylonitrile adsorbate does not depend significantly on the size of the metal clusters,[19] and (ii) the chemical potential of the metal clusters, relevant for determining the direction of the partial charge transfer upon chemisorption, is quasi-constant with cluster size and very close to the bulk value, as we showed earlier.[16]

The choice of small clusters to model metal surfaces needs justification because numerous studies have shown that the chemisorption energy of an adsorbate interacting with metal clusters (which model an adsorption site on a metal surface) oscillates with cluster size, cluster shape, and adsorption site

(9) Nüesch, F.; Kamarás, K.; Zuppiroli, L. *Chem. Phys. Lett.* **1998**, *283*, 194.
(10) Campbell, I. H.; Kress, J. D.; Martin, R. L.; Smith, D. L.; Barashkov, N. N.; Ferraris, J. P. *Appl. Phys. Lett.* **1997**, *71*, 3528.
(11) Zehner, R. W.; Parsons, B. F.; Hsung, R. P.; Sita, L. R. *Langmuir* **1999**, *15*, 1121.
(12) Krüger, J.; Bach, U.; Grätzel, M. *Adv. Mater.* **2000**, *12*, 447.
(13) See http://www.ifm.liu.se/Surfphys/equipment/scienta1.jpg for details.
(14) (a) Velde, G. t.; Baerends, E. J. *Chem. Phys.* **1993**, *177*, 399. (b) Hermann, K.; Bagus, P. S.; Nelin, C. J. *Phys. Rev. B* **1987**, *35*, 9467. (c) Mijoule, C.; Baba, M. F.; Russier, V. *J. Mol. Catal.* **1993**, *83*, 367.
(15) (a) Panas, I.; Schüle, J.; Siegbahn, P.; Wahlgren, U. *Chem. Phys. Lett.* **1988**, *149*, 265. (b) Klopman, G.; Hudson, R. F. *Theor. Chim. Acta* **1967**, *8*, 165.
(16) Crispin, X.; Geskin, V.; Lazzaroni, R.; Bureau, C.; Brédas, J. L. *Eur. J. Inorg. Chem.* **1999**, *349*, 9.
(17) Crispin, X.; Lazzaroni, R.; Geskin, V.; Baute, N.; Dubois, P.; Jérôme, R.; Brédas, J. L. *J. Am. Chem. Soc.* **1999**, *121*, 176.
(18) Trasatti, S. *Electrochim. Acta* **1992**, *37*, 2137.
(19) Crispin, X.; Geskin, V.; Lazzaroni, R.; Bureau, C.; Salaneck, W.; Brédas, J. L. *J. Chem. Phys.* **1999**, *111*, 3237.

on the cluster. The magnitude of these oscillations can be dramatic (i) when the adsorbate interacts with the cluster via a single site, a single bond, and (ii) with small quasi-spherical metal clusters. For CO on Cu_n[14a,b] (Ni_n[14c]) clusters, the chemisorption energy can change nonmonotonically by 20 kcal/mol (40 kcal/mol) with cluster size. These oscillations arise from the discrete electronic configuration of finite metal clusters;[15a] the nature of frontier orbitals changes with size, so their shape can be more or less favorable for chemisorption in different clusters. However, the chemisorption energy oscillations versus cluster size are significantly damped for (i) relatively large, π-conjugated molecular adsorbates interacting with the metal cluster via several moieties, several chemical bonds, and (ii) large and flat metal clusters. Fortunately, this is the case for AN interacting with two-layer copper clusters; for $Cu_n(100)$ with $n = 9-20$, we have found that the evolution of the binding energy with cluster size displays a rather weak oscillation with a magnitude of ca. 8 kcal/mol.[19] The reason for this behavior is well understood. First, the use of large and flat metal clusters, rather than small and quasi-spherical ones, provides a metal electronic structure free of electronic shell structure and close to the density of states of the actual metal surface.[16] Second, the presence of two (rather than one) interaction sites for AN on the clusters via two chemical moieties (the C═C double bond and the C≡N nitrile group) is also susceptible to damp the oscillations. In addition, the geometry of the acrylonitrile adsorbate does not depend significantly on the size of the metal clusters.[19] Therefore, nine-atom flat clusters appear as a reasonable model for AN adsorption on metal surfaces.

The interatomic distances in the clusters are fixed at the bulk values. The geometric structures of Ni_9 and Cu_9 are similar; the distance between the central atom of the upper layer and the other atoms is 2.49 Å for Ni and 2.55 Å for Cu. The first layer of Fe_9 is less densely packed than those in Ni_9 and Cu_9, the distance between the central atom and other atoms of this layer being 2.87 Å. The (100) surface is chosen because it presents similar structures for the fcc lattice of Ni and Cu and for the more open bcc structure of Fe. Moreover, the (100) surface has a surface atomic density intermediate between that of the compact (111) surface and that of the open (110) surface; because the reactivity of the surface depends on surface atomic density,[18] the (100) surface can be considered as possessing an average reactivity of different faces of the polycrystalline metal surface.

3.2. Methodology. Transition metal clusters can be accurately described by means of quantum-mechanical methods based on density functional theory (DFT).[20] These methods include a significant part of the electron correlation energy, which is essential for a correct description of transition metal compounds. The DFT calculations were performed with the DMol program.[21,22] The chosen basis set is DNP (double-ζ numeric with polarization). The core orbitals are frozen during the self-consistent field (SCF) iterations, and a fine mesh size is used for the calculations.[21,22] Geometry optimizations are carried out with the eigenvector-following algorithm by Baker,[23] within the local spin density approximation (LSD), using the Vosko−Wilk−Nusair exchange-correlation potential.[24] This algorithm was improved to optimize the geometry in Cartesian coordinates[25] and to introduce constraints (fixed atoms) in Cartesian coordinates thanks to an efficient Lagrange multiplier algorithm.[26] The geometry optimizations are unconstrained except for the distances between metal atoms that are kept at the bulk crystal values. The starting geometry of AN is flat on the surface of the cluster. The LSD approximation is known to provide reliable adsorption geometries of adsorbates.[17,27] To characterize qualitatively the partial charge transfer upon chemisorption, the Mulliken atomic charges are used.

Note that the SCF procedure used to minimize the ground-state energy shows strong oscillations in electron density and total energy. This oscillation problem is well known in systems having a vanishing HOMO−LUMO gap because of the symmetry of the system or because of d molecular orbitals very close to each other in energy, as can be the case in transition metal clusters. To overcome this difficulty, we have followed the method proposed by Rabuck et al.[28] to reach convergence, one allows molecular orbitals to be fractionally occupied. Here, the valence electrons are spread over an energy window, that is, a range of molecular orbital energies broader than that given by a Fermi−Dirac distribution at 0 K. The calculations are then performed in several steps, starting in the first step with a large energy window. At each step, the SCF convergence is reached; then, the size of the window is reduced. Finally, the last step corresponds to zero temperature and gives integer orbital occupations at convergence.

4. Results

4.1. Structure of AN Chemisorbed on the Metal Surfaces: Theoretical Results. Figure 2 and Table 1 collect the main results. Figure 2a sketches the adsorption structure of AN on a Cu(100) surface modeled with a nine-atom copper cluster. The C═C and C≡N groups are asymmetrically coordinated to each one copper atom. Two copper atoms show distances with AN atoms indicating the formation of chemical bonds; the shortest contacts are with the two terminal backbone atoms (C^1 and N): the distance between C^1 and the central copper atom is 2.08 Å, and that between the nitrogen atom and the closest copper atom is 1.89 Å. The distances with the other two carbon atoms are 2.49 and 2.37 Å, see Table 1. The adsorption of AN on copper appears to occur through the formation of di-σ-complexes. The major changes in bond length for AN in the complexes, relative to the isolated molecule, are significant elongations of the C^1-C^2 and C^3-N bonds, while C^2-C^3 assumes a double-bond character. The reason for this geometric rearrangement is related to the lower availability of the 2p electrons of the C and N terminal atoms for the π-system, because of their involvement in bonding with copper, and a new π-bond is formed between the two central carbon atoms. As a result, the C^2C^3N bond angle deviates from 180°, which can be interpreted as a change in apparent hybridization of all backbone atoms. Another feature indicating the change in hybridization, from sp^2 to sp^3, of the C^1 atom is the positions of the adjacent hydrogen atoms, which shift away from the plane

(20) Parr, R. G.; Yang, W. *Density-Functional Theory of Atoms and Molecules*; Oxford University Press: New York, 1989.
(21) Delley, B. *J. Chem. Phys.* **1990**, *92*, 508.
(22) Delley, B. *New J. Chem.* **1992**, *16*, 1103.
(23) Baker, J. *J. Comput. Chem.* **1986**, *7*, 385.
(24) Vosko, H.; Wilk, L.; Nusair, M. *Can. J. Phys.* **1980**, *58*, 1200.
(25) Baker, J.; Hehre, W. J. *J. Comput. Chem.* **1991**, *12*, 606.
(26) Baker, J. *J. Comput. Chem.* **1993**, *14*, 1085.
(27) Ziegler, T. *Chem. Rev.* **1991**, *91*, 651.
(28) Rabuck, A. D.; Scuseria, G. E. *J. Chem. Phys.* **1999**, *110*, 695.

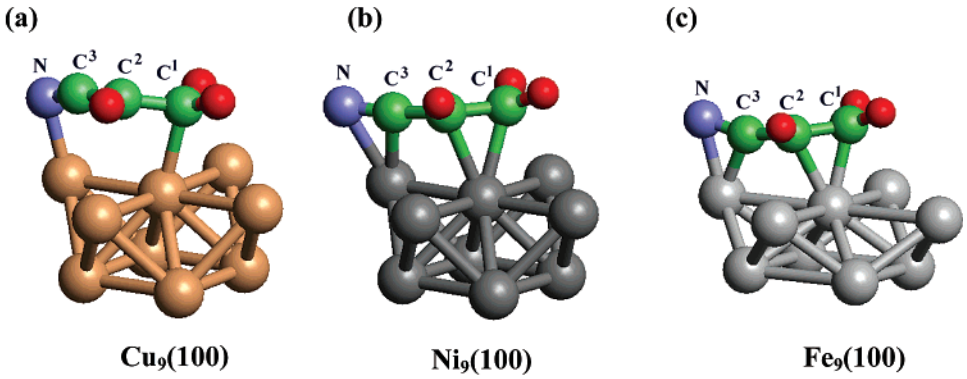

Figure 2. Sketch of the optimized structures of AN on (a) a nine-atom copper cluster modeling an adsorption site of the Cu(100) surface, (b) a nine-atom nickel cluster simulating the Ni(100) surface, and (c) a nine-atom iron cluster simulating the Fe(100) surface.

Table 1. Selected Structural Parameters for the [AN−M_9] Complexes with M = Cu, Ni, and Fe[a]

	C^1C^2	C^2C^3	C^3N	C^1M	C^2M	C^3M^*	NM*	C^2C^3N	*q*(AN)
AN	1.336	1.410	1.169					180	0
[AN−Cu_9]	1.427	1.362	1.201	2.08	2.49	2.37	1.89	166	−0.18
[AN−Ni_9]	1.448	1.447	1.222	2.12	2.17	1.98	2.10	168	−0.26
[AN−Fe_9]	1.421	1.418	1.239	2.00	2.06	1.85	1.90	160	−0.30

[a] The interatomic distances are in Å, the angle C^2C^3N is in degrees, and the Mulliken atomic charge carried by AN, *q*(AN), is in |e|. The central atom on the metal surface is noted M*, while the edge-atom involved in the chemisorption is noted M.

of the molecule. We emphasize that similar adsorption geometries are found when increasing the size of the copper surface from 9 to 20 atoms.[19]

AN is found to adsorb flat on a specific adsorption site of the Ni(100) and Fe(100) surfaces (see Figure 2b and c, respectively). The distances between the backbone atoms of AN and the metal atoms involved in the chemisorption range between 1.98 and 2.17 Å for nickel (1.85 and 2.06 Å for iron), which indicates that here all the carbon atoms are involved in the chemisorption process. Consequently, these chemisorptions follow a di-π-adsorption process where the $2p_\pi$ atomic orbitals originally involved in the C^1-C^2 and C^3-N bonds now interact with the 3d and 4s atomic orbitals of Ni and Fe. For nickel, the C^1-C^2, C^2-C^3, and C^3-N bonds all elongate, by 0.11, 0.04, and 0.05 Å, respectively. The same trend is observed for iron, where the corresponding elongations are 0.09, 0.01, and 0.07 Å. The only difference between nickel and iron seems to be the larger stretching of the nitrile group, while the central C^2-C^3 bond length is hardly affected. The involvement of the $2p_\pi$ electrons in the interfacial bonds leads to a change in the hybridization of the AN backbone atoms; this is reflected by the C−H bonds tilting away from the plane of the double bond and the C^2-C^3-N group presenting an angle of 168°, instead of 180° in the isolated molecule. A similar adsorbate structure is obtained when AN interacts with a 16-atom nickel cluster.[17] Although the difference between the adsorption on copper (di-σ), on one side, and nickel and iron (di-π), on the other side, is not fully understood, it is likely because of the fact that the 3d orbitals are fully occupied for copper, while partially occupied for iron and nickel.

Upon chemisorption, the atomic charge distribution is significantly modified over the adsorbate. That is mainly because of a partial charge transfer with the metals and the formation of new chemical covalent bonds with the metal surface as well as because of the structural change of the molecule. To isolate the second effect, the Mulliken atomic charge distribution has been calculated for the neutral isolated AN molecule in the geometry found in the [AN−M_9] complexes. Table 2 displays the carbon and nitrogen atomic Mulliken charges for the distorted AN molecule corresponding to AN in complexes [AN−Fe_9], [AN−Ni_9], and [AN−Cu_9], as well as for the neutral AN molecule before chemisorption. It is seen that the distortions because of complexation have little influence on the atomic charge distribution on individual carbon atoms, and influence even less the average charge on the carbon atoms [$C^1 + C^2 + C^3$/3]; the latter is related to the average binding energy of the three C(1s) contributions (Figure 3) discussed in the XPS section 4.2. Similarly, no significant change is found for the charge carried by the nitrogen atom. These results suggest that the structural change of the adsorbate upon chemisorption does not play a major role in the atomic distribution change upon chemisorption. Therefore, it is the formation of the new chemical bonds with the metal atoms leading to partial charge transfer (rather than the structural distortion of the adsorbate upon chemisorption) that is responsible for a major change in electronic density over the chemisorbed AN molecule.

Table 2. Net Mulliken Atomic Charges, in |e|, Carried by the Carbon and Nitrogen Atoms in (i) Neutral AN in Its Optimized Structure and (ii) Neutral AN in the Structure It Adopts When Chemisorbed on the Copper, Nickel, and Iron Cluster[a]

atoms	AN	AN in [AN–Fe_9]	AN in [AN–Ni_9]	AN in [AN–Cu_9]
C^1	−0.523	−0.568	−0.563	−0.563
C^2	−0.189	−0.219	−0.240	−0.224
C^3	0.012	0.040	0.041	0.051
$(C^1 + C^2 + C^3)/3$	−0.233	−0.249	−0.254	−0.245
N	−0.179	−0.200	−0.192	−0.198
μ_A (eq 3b)	−5.50 eV	−5.60 eV	−5.67 eV	−5.55 eV

[a] The last row gives the chemical potential of the AN molecule in the different structures.

The Mulliken charge *q*(AN) carried by AN is smaller on the copper surface (−0.18 |e|) than it is on the nickel (−0.26 |e|) and iron (−0.30 |e|) surfaces. It must be kept in mind that these values give simply an indication about the relative importance of charge transfer for the three metals (the absolute magnitudes

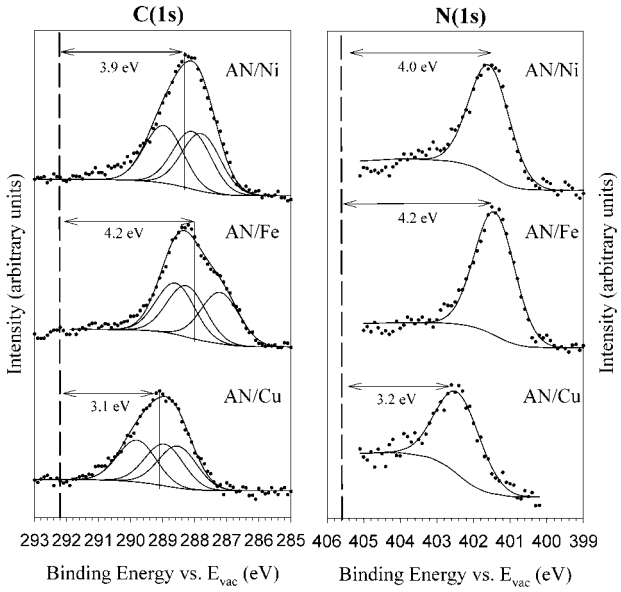

Figure 3. C(1s) (left) and N(1s) (right) spectra of AN monolayers chemisorbed on Ni, Fe, and Cu. The dashed lines indicate the positions of the peaks of AN in the gas phase. The binding energies refer to the vacuum level. The C(1s) peak position is given by the average binding energy of the three carbon components.

should be considered cautiously, as they are related to an arbitrary partitioning scheme).

4.2. Partial Charge Transfer upon Chemisorption on the Basis of XPS. Partial charge transfer upon chemisorption can be investigated experimentally via XPS, because an increase in electron density on the adsorbate gives rise to a lower binding energy of its core electrons. AN has been adsorbed on three transition metal surfaces: Cu, Ni, and Fe as described in the Experimental Section. Figure 3 shows the C(1s) and N(1s) spectra of the chemisorbed monolayers obtained by adsorption at −90 °C. The C(1s) and N(1s) spectra for AN/Cu appear at higher binding energies relative to AN/Ni and AN/Fe, which suggests that the chemical interaction between the molecule and the metal is different on copper as compared to nickel and iron. This difference in behavior is consistent with the theoretical results discussed in the previous section that indicate that the interaction of acrylonitrile on Cu(100) is a di-σ-chemisorption process, while a di-π-chemisorption is observed on Ni(100) and Fe(100).

To evaluate experimentally the partial charge transfer upon chemisorption, we use the positions of the C(1s) and N(1s) peaks in Figure 3 and compare them to the gas-phase values (because three nonequivalent carbon atoms are present in AN, the position of the C(1s) peak is determined by the average energy of the three C(1s) components). A large shift on the order of 3−4 eV appears between the C(1s) and N(1s) binding energies measured for the chemisorbed monolayer (with respect to the vacuum level) and the gas-phase values.[29,30] It is important to note that this binding energy shift, ΔEb, for AN going from the gas phase to an adsorbed monolayer situation, is not exclusively because of the rearrangement of the electron density upon chemisorption. Several other effects, that will be detailed below, do contribute: (i) the polarization energy because of the metal, $E_{pol}{}^{m}$; (ii) the polarization energy because of the surrounding AN molecules, $E_{pol}{}^{AN}$; and (iii) the surface dipole effect, efD_{met}, where fD_{met} is a fraction of the metal surface dipole potential D_{met}. Hence, to obtain the "chemical" effect contribution, ΔE_{chem}, because of the partial charge transfer, the other contributions must be evaluated. The core binding energy for AN in the gas phase, Eb_{gas}, can be compared to the measured Eb_{mono} for a chemisorbed AN monolayer (referred to the vacuum level by adding the work function of the sample) via the relation:[31]

$$\Delta Eb = Eb_{gas} - Eb_{mono} = E_{pol}{}^{m} + E_{pol}{}^{AN} - efD_{met} + \Delta E_{chem} \quad (1)$$

Here, we make the approximation that these effects are additive and independent from each other; this is true only to a certain extent. Therefore, the evaluation of all the terms as proposed below must be considered as semiquantitative. Note that the polarization of the electronic cloud of an adsorbate because of the interaction between the adsorbate electrons and their image charges on the metal surface side is expected to produce only a small dipolar energy contribution in eq 1, estimated to be 0.1 eV for Xe on Ag.[32] We therefore neglect this effect in the remainder of the discussion.

A significant screening contribution of the core-hole arises from the metal surface. The attractive potential felt by a charge (core-hole) in front of a metal surface is usually estimated by a classical image potential (see, e.g., ref 33) or within the dielectric continuum model.[34] However, these potentials present the drawback that they have no physical meaning close to the metal surface (because they tend to $-\infty$); as a result, they cannot be used to estimate the metal polarization energy $E_{pol}{}^{m}$ for a hole created by photoionization in a chemisorbed molecule that is very close to the metal. On approaching the metal surface, the electronic exchange-correlation contributions become important, and the potential, called the effective potential v_{eff} in DFT, must merge smoothly with the crystal potential. Such a feature is taken into account with the Jones−Jennings−Jepsen (JJJ) potential (eqs 2a and b), which fits well with the effective potential obtained by DFT calculations:[35,36]

$$V_{JJJ}(d) = \frac{-1}{2\epsilon(d - x_{im})}[1 - \exp(-\lambda(d - x_{im}))]; \quad d > x_{im} \quad (2a)$$

$$V_{JJJ}(d) = \frac{-v_{eff}}{A\exp(B(d - x_{im})) + 1}; \quad d < x_{im} \quad (2b)$$

where x_{im} is the image plane position defining the effective location of the metal surface. In the region from the effective metal plane toward the adsorbate ($d > x_{im}$), the metal polarization energy for a photoelectron leaving the adsorbate is a decreasing exponential given by $E_{pol}{}^{m} = V_{JJJ}(d)$ (eq 2a) and characterized by λ. The parameters of this potential have been determined for copper and nickel: $x_{im} = 2.33$ and 2.37, $v_{eff} = 0.54$ and 0.59, and $\lambda = 1.17$ and 1.21, in atomic units, for

(29) Brito, A. N. d.; Svensson, S.; Agren, H.; Delhalle, J. *J. Electron Spectrosc. Relat. Phenom.* **1993**, *63*, 239.
(30) Bureau, C.; Chong, D. P.; Lécayon, G.; Delhalle, J. *J. Electron Spectrosc. Relat. Phenom.* **1997**, *83*, 227.
(31) (a) Gadzuk, J. W. *Phys. Rev. B* **1976**, *14*, 2267. (b) Lang, N. D.; Williams, A. R. *Phys. Rev. B* **1982**, *25*, 2940.
(32) Lang, N. D. *Phys. Rev. Lett.* **1981**, *46*, 842.
(33) Kaindl, G.; Chiang, T. C.; Eastman, D. E.; Himpsel, F. J. *Phys. Rev. Lett.* **1980**, *45*, 1808.
(34) Hotzel, A.; Moos, G.; Ishioka, K.; Wolf, M.; Ertl, G. *Appl. Phys. B* **1999**, *68*, 615.
(35) Jones, R. O.; Jennings, P. J.; Jepsen, O. *Phys. Rev. B* **1984**, *29*, 6474.
(36) Smith, N. V.; Chen, C. T.; Weinert, M. *Phys. Rev. B* **1989**, *40*, 7565.

Cu(100) and Ni(100), respectively.[35,36] The dielectric constant ϵ introduced in the JJJ potential models the decrease in electrostatic attraction between the hole and the induced image charge at the metal surface because of the electron density of the valence states of the adsorbate localized between the core-hole and the metal surface. For Xe on Pd(100), the JJJ potential with $\epsilon = 2$ matches the experimental results obtained for the metal polarization energy.[37] Even though Xe and AN are rather different systems, using $\epsilon = 2$ should give the correct order of magnitude for this dielectric effect of the valence electron density of the AN molecule. From the calculated structures, the carbon and nitrogen atoms of the AN adsorbate are at 1.9 Å from the surface atoms. Introducing $\epsilon = 2$ and $d = 1.9$ Å in eq 2a gives a metal screening energy of $E_{pol}^{m} = 2.3$ eV for both Cu and Ni. From a photoelectron spectroscopic study of Xe adsorbed on different metals, Chiang et al. demonstrated that the metal screening does not depend significantly on the nature of the metal surfaces.[38] Thus, the metal polarization energy E_{pol}^{m} for a chemisorbed AN monolayer on Fe is also considered to be equal to 2.3 eV.

The AN molecules surrounding the core-hole created by photoionization of an adsorbate molecule also contribute to its screening. The polarization energy of AN in a monolayer, E_{pol}^{AN}, is estimated to be 0.6 eV. This has been found from an XPS investigation of an AN bilayer.[39] The C(1s) and N(1s) core-electron binding energies of the top layer of an AN bilayer are shifted by 1.7 eV with respect to the binding energies obtained from XPS in the gas phase.[39] Hence, for the top layer of a bilayer, $E_{pol}^{m} + E_{pol}^{AN} = 1.7$ eV. The metal polarization energy E_{pol}^{m} for the top layer is estimated to be 0.5 eV; this is obtained from eq 2a with a distance $d = 5.2$ Å between the metal surface and the AN nuclei in the top layer (assuming that the molecules in the second layer are parallel to the chemisorbed layer). The effect of the first adsorbed layer on the screening of the metal is taken into account by considering a dielectric constant $\epsilon = 2$, as discussed above. E_{pol}^{AN} for the top layer of the bilayer is therefore equal to 1.2 eV. A simple approximation is to consider that the molecules, within the top layer and within the bottom layer, contribute equally to the AN polarization energy. Following this assumption, the polarization effect within an AN monolayer, E_{pol}^{AN} in eq 1, is $^1/_2E_{pol}^{AN}$ for a bilayer, that is, $^1/_2 1.2 = 0.6$ eV. We note that these polarization effects, E_{pol}^{AN} and E_{pol}^{m}, contribute to *decrease* the core-electron binding energies measured with XPS with respect to the gas-phase values.

A neutral metal surface in a vacuum presents a surface dipole because there occurs a deficit of electronic density $\rho(x)$ (bottom dotted curve, Figure 4) inside the metal close to the surface, while an excess of electronic density is obtained outside the surface. As a consequence, the electrostatic potential $\phi(x)$ (top full line, Figure 4) jumps from its bulk value ϕ^{in} (inner potential) to a higher value ϕ^{out} outside the metal (outer potential). The difference between the inner and outer electrostatic potentials defines the metal surface dipole potential energy, $eD_{met} = e(\phi^{out} - \phi^{in})$, which can reach several electronvolts. The surface dipole potential energy has been evaluated by Lang as the difference between the calculated DFT bulk chemical potential and the experimental work function; it is calculated to be 3.6 eV for Cu, 4.2 eV for Ni, and 4.9 eV for Fe.[40] These values seem reasonable, according to what is found in section 4.4.2 below.

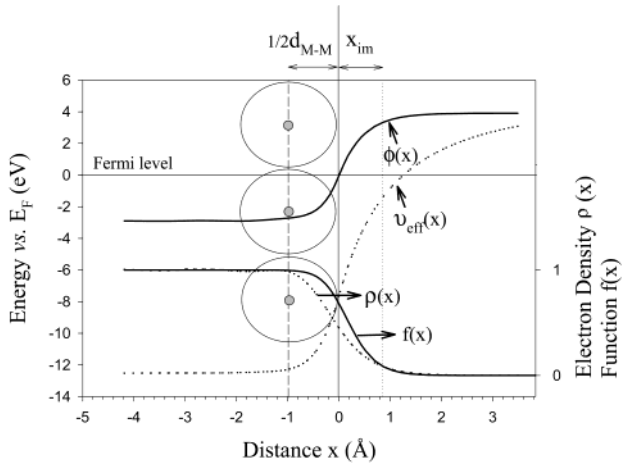

Figure 4. DFT calculations within the jellium model by Lang and Kohn[40] give the evolution of the electron density $\rho(x)$ across the metal/vacuum interface (bottom dotted curve), the effective potential $\upsilon_{eff}(x)$ (top dotted curve), and the electrostatic potential $\phi(x)$ (top solid line). As explained in the Appendix, the function $f(x)$, used to estimate the contribution efD_{met} in eq 1, can be fitted with the sigmoid function plotted in as a solid at the bottom. The large circles depict the atoms on the metal surface; the zero on the x axis is positioned at one-half the interatomic layer distance ($^1/_2d_{M-M}$) from the surface nuclei plane ($x > 0$ indicates the metal bulk); x_{im} defines the image plane position used in eq 2.

The evolution of the electrostatic potential $\phi(x)$ across the metal/vacuum interface is related to the difference between the electron density $\rho(x)$ and the nucleus density. In the jellium model, the nucleus density is represented by a step function; that is, the nucleus density drops to zero at the metal surface (the jellium edge). On the other hand, the electron density of a metal surface decreases exponentially over several angströms[41] away from the surface plane of the metal nuclei, that is, well beyond the position of the nuclei of the AN adsorbate (~1.9 Å). As a result, the electrostatic potential outside the metal has a behavior opposite to the electron density; if the zero energy is set at E_F, $\phi(x)$ tends exponentially to the work function, see Figure 4.

When one AN molecule approaches the surface, it enters into the electrostatic field because of the surface dipole; this contributes to *increase* the binding energy of the core-electrons by a value $f(x)eD_{met}$,[32] where x defines the position of the adsorbate with respect to the metal surface plane. Lang and Williams have confirmed from their DFT calculations performed on a jellium metal−adsorbate system that the variation of the deep core eigenenergies with metal−adsorbate distance follows the bare-metal electrostatic potential $\phi(x)$ rather than the total bare-metal potential, that is, the effective potential $\upsilon_{eff}(x)$ (top dotted curve, Figure 4).[42] Note that the electrostatic potential does not extend as far outside the metal as does the effective potential,[43] such that the contribution feD_{met} in eq 1 is always smaller than the contribution E_{pol}^{m} directly estimated from the effective potential $\upsilon_{eff}(x)$.

(37) Wandelt, K.; Hulse, J. E. *J. Chem. Phys.* **1984**, *80*, 1340.
(38) Chiang, T. C.; Kaindl, G.; Mandel, T. *Phys. Rev. B* **1986**, *33*, 695.
(39) Crispin, X.; Andersson, A.; Lazzaroni, R.; Brédas, J.-L.; Salaneck, W. *J. Electron Spectrosc. Relat. Phenom.* **2001**, *121*, 57.
(40) Lang, N. D. DFT Approach to the Electronic Structure of Metal Surfaces and Metal−Adsorbate Systems. In *Theory of the Inhomogeneous Electron Gas*; Lundqvist, S., March, N. H., Eds.; Plenum Press: New York, 1983.
(41) Lang, N. D.; Kohn, W. *Phys. Rev. B* **1973**, *7*, 3541.
(42) Lang, N. D.; Williams, A. R. *Phys. Rev. B* **1978**, *18*, 616.
(43) Lang, N. D.; Kohn, W. *Phys. Rev. B* **1970**, *1*, 4555.

To our knowledge, no analytical form of $f(x)$ is available for Cu, Ni, and Fe. To estimate the order of magnitude of the contribution $f(x)eD_{met}$ in eq 1 for AN chemisorbed on those metals, a jellium model with an electron density characterized by a Wigner−Seitz radius (radius of a sphere whose volume is equal to the volume per conduction electron) $r_s/a_0 = 2$, close to the electron density in Cu, Ni, and Fe,[44] is used. For such metals, DFT calculations within the jellium model give the evolution of the electron density $\rho(x)$ (bottom dotted curve), the effective potential $v_{eff}(x)$ (top dotted curve), and the electrostatic potential $\phi(x)$ (top full line) displayed in Figure 4 (data by Lang and Kohn[43]). As explained in the Appendix, the function $f(x)$ can be fitted with the sigmoid function plotted in Figure 4 (bottom full line). We believe that this function $f(x)$ provides a reasonable value for the fraction of the total metal surface dipole potential energy $f(x)eD_{met}$ that has to be taken into account in eq 1. Considering eD_{met} equal to 3.6 eV for Cu, 4.2 eV for Ni, and 4.9 eV for Fe[40] and a value $f(1.9\ \text{Å}) = 0.05$ for AN chemisorbed at $x = 1.9$ Å from the plane of metal surface nuclei (see Appendix), we found that the contribution efD_{met} amounts to 0.18 eV for Cu(100), 0.21 eV for Ni(100), and 0.24 eV for Fe(100). Such small values indicate that the core electrons of large π-conjugated organic molecules, chemisorbed via several metal surface atoms on a compact surface, are not going to see their binding energy raised significantly by the electrostatic potential of the metal surface. In contrast, small atoms are expected to occupy hollow sites and to be within the electrostatic surface metal dipole; as a result, the binding energy of the core electrons of small adsorbates can be raised significantly by efD_{met}. In the case of physisorbed molecules or atoms, the electrons of the adsorbate are far enough from the surface that they do not significantly feel the electrostatic potential of the metal surface, and efD_{met} is zero. Note that the mere presence of an adsorbate close to the metal surface induces a change in the surface metal dipole, which diminishes the efD_{met} contribution. As discussed in section 4.4.2, a work function change (or, in other words, a metal surface dipole change) of 0.6 eV is observed upon adsorption of Xe on Cu and Fe (see Figure 6). The result for Xe gives a rough estimate for the modification of the correction efD_{met} to be taken into account when the surface metal dipole changes upon adsorption of AN; decreasing D_{met} by 0.6 eV gives a contribution efD_{met} equal to 0.15 eV for Cu(100), 0.18 eV for Ni(100), and 0.21 eV for Fe(100) (assuming that the f function is similar in all cases).

Table 3 displays the estimates of the contributions to the chemical shifts because of partial metal−adsorbate charge transfer, ΔE_{chem}, as obtained from eq 1. For all of the metals, the estimated chemical shift turns out to be very similar for N(1s) and C(1s). Its sign is positive, which implies that the electron density around the carbon and nitrogen atoms is increased upon chemisorption. In other words, there is a partial electron transfer from the metal surface to the AN molecule. The chemical shifts of C(1s) and N(1s) indicate that the carbon and nitrogen atoms are all involved in the chemisorption process; this is consistent with the theoretical results (Figure 2) showing a preferential chemisorption of AN flat on the copper, iron, and nickel surfaces[17,19,39,45] via both the C═C double bond and the nitrile group. Note that other experimental studies indicate a similar chemisorption geometry of acrylonitrile on various metals: Ag,[46] Cu,[47] Au electrodes,[48,49] and Pt(111).[50]

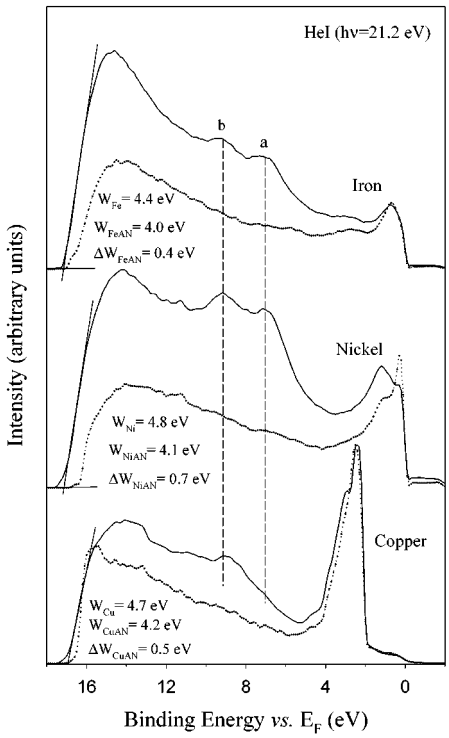

Figure 5. Comparison between the UPS HeI spectra of the clean metal surface (dotted line) and the spectra obtained after adsorption of an AN monolayer at −90 °C (full line). The spectra are normalized to the maximum intensity of the valence features. Peaks a and b indicate some electronic levels of the chemisorbed acrylonitrile.

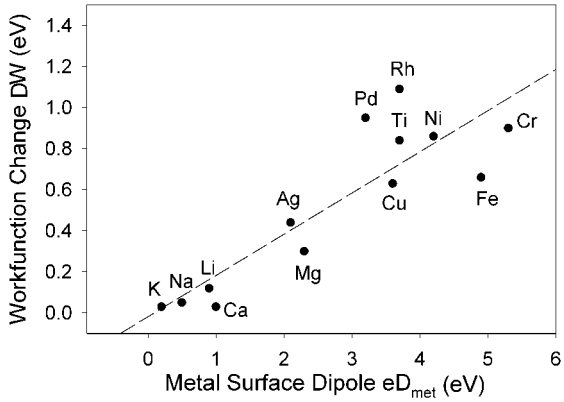

Figure 6. Evolution of the work function change (data from ref 67) of various metals upon adsorption of a Xe monolayer, with respect to the metal surface dipole (data from ref 37).

Table 3. Values of the Energetic Contributions (in eV) Appearing in Eq 1[a]

	C(1s)	N(1s)	C(1s) ΔEb	N(1s) ΔEb	C(1s) ΔE_{chem}	N(1s) ΔE_{chem}
Cu	289.1	402.4	3.1	3.2	0.4	0.5
Ni	288.3	401.6	3.9	4.0	1.2	1.3
Fe	288.0	401.4	4.2	4.2	1.5	1.5
AN gas	292.2	405.6				

[a] Note that the C(1s) and N(1s) peak positions refer to the vacuum level.

(44) Ashcroft, N. W.; Mermin, N. D. *Solid State Physics*; Saunders College Publishing: Fort Worth, 1976.
(45) Geskin, V.; Lazzaroni, R.; Mertens, M.; Jérome, R.; Brédas, J. L. *J. Chem. Phys.* **1996**, *105*, 3278.
(46) Xue, G.; Dong, J.; Zhang, J.; Sun, Y. *Polymer* **1994**, *35*, 723.
(47) Loo, B. H.; Kato, T. *Surf. Sci.* **1993**, *284*, 167.

Even though the XPS chemical shifts are known to be related to the atomic charges,[51,52] attempts to correlate directly C(1s) and N(1s) binding energies and atomic charges face several difficulties.[52−54] However, here, the same molecule is considered, and the metal screening is expected to be similar for Cu, Ni, and Fe. Thus, we believe that the estimated chemical shift ΔE_{chem} can be directly related to the partial charge transfer from the metal surfaces to the chemisorbed AN molecules. ΔE_{chem} is then directly related to the chemical nature of the metal. Table 3 clearly displays the difference between, on one hand, nickel and iron and, on the other hand, copper. The small chemical shift [0.4 eV for C(1s) and 0.5 eV for N(1s)] observed for AN chemisorbed on copper as compared to the other two metals [around 1.3 eV for both C(1s) and N(1s) with nickel and 1.5 eV with iron] indicates that the partial charge transfer upon chemisorption is lower with Cu than with Ni and Fe. This is fully consistent with the results from our DFT calculations modeling the AN chemisorption on metal clusters; the charge carried by AN is negative and smaller when the molecule is chemisorbed on Cu_9(100) than on the Ni_9(100) and Fe_9(100) surfaces (see Table 1).

A consequence of the partial charge transfer between the chemisorbed molecules and the metal surface is the formation of a "chemical" dipole potential, D_{chem}, with the positive side of the dipole pointing toward the metal surface and the negative pole in the AN adsorbates.

4.3. Partial Charge Transfer upon Chemisorption: A DFT Approach. The chemical dipole potential D_{chem} only appears for chemisorption, that is, when there occurs a significant overlap and rearrangement of the electron densities between the adsorbate and the metal adsorption site. The rearrangement of the electron density on the adsorbate is seen as a partial charge transfer. The formation of chemical bonds accompanied with a partial charge transfer is a well-known chemical concept early described as the Sanderson principle of electronegativity equalization.[55] Nowadays, this phenomenon is fully rationalized in DFT and described with the concept of electronic chemical potential. When two systems (in our case, a metal surface and an organic molecule) interact, their electronic chemical potentials tend to equalize; this determines the direction of electron transfer.[56,57] The charge goes from the species with the higher chemical potential toward that with the lower chemical potential.

The chemical potential μ of a molecule is the derivative of the electronic energy E relative to the number of electrons N (eq 3a). In molecules, it can be estimated (from the so-called finite-difference approximation) as minus the average of the first ionization potential (IP) and the electron affinity (EA),[58,59] eq 3b (note that this corresponds to the opposite of Mulliken's formula for electronegativity[60]); for metals, the DFT chemical potential is the opposite of the work function,[61,62] eq 3c:

$$\mu = \left(\frac{\partial E}{\partial N}\right)_{v_{ext}} \tag{3a}$$

For molecules:

$$\mu_A \cong -\frac{IP + EA}{2} \tag{3b}$$

For metals:

$$\mu_m \cong -W \tag{3c}$$

The derivative in eq 3a is carried out at constant external potential $v_{ext}(r)$, equal to the electron-nuclei potential plus any other potential applied to the system. Hence, from three experimental parameters, the work function of the bare metal W and the ionization potential IP and electron affinity EA of the isolated adsorbate, the direction of the charge transfer, and the orientation of the dipole associated to the chemical dipole potential D_{chem} can be predicted. To investigate the validity of using the principle of equalization of the chemical potentials, we analyze next the influence of the nature of the metal on the partial charge transfer upon chemisorption, using our data for AN chemisorbed on Cu, Ni, and Fe.

From our DFT calculations (section 4.1), the chemical potentials of the metal clusters given by the HOMO energy, ϵ_{HOMO},[17] are calculated to be $\mu^{DFT}_{Cu} = -\epsilon_{HOMO}(Cu_9) = -4.3$ eV, $\mu^{DFT}_{Ni} = -4.0$ eV, $\mu^{DFT}_{Fe} = -4.0$ eV. The experimental chemical potentials of the metal surfaces are the opposite of the work functions (eq 3c): $\mu_{Cu} = -4.7$ eV, $\mu_{Ni} = -4.8$ eV, $\mu_{Fe} = -4.4$ eV. Thus, the small metal clusters have a chemical potential close to the metal work function; as a result, they are expected to give the correct direction for the charge transfer with an adsorbate. The chemical potentials of Cu, Ni, and Fe are found to be higher than the chemical potential of the AN isolated molecule. From eq 3b, the calculated chemical potential of AN is −5.50 eV; this is in good agreement with the experimental chemical potential (−5.45 eV) obtained from the experimental ionization potential (10.91 ± 0.01 eV)[63] and electron affinity (0.02 ± 0.01 eV).[64,65] The chemical potential of the neutral isolated AN adsorbate, in the structure it has in the [AN−M_9] complexes, is calculated from eq 3b and reported in Table 2. The chemical potential of AN in the distorted structure is only about 0.1 eV lower than that for the isolated AN molecule prior to chemisorption. Thus, the structural change upon chemisorption should not affect the prediction for the direction of partial charge transfer given by the 1 eV chemical potential difference between the metal and the adsorbate. Clearly, the chemical potential equalization is expected to produce a partial electron transfer from the metal surface to the AN adsorbate. This is fully consistent with the XPS chemical shift ΔE_{chem} estimated for a chemisorbed AN monolayer (see

(48) Bewick, A.; Gibilaro, C.; Razag, M.; Russell, J. W. *J. Electron Spectrosc. Relat. Phenom.* **1983**, *30*, 191.
(49) Gao, P.; Weaver, M. J. *J. Phys. Chem.* **1985**, *89*, 5040.
(50) Parent, P.; Laffon, C.; Tourillon, G.; Cassuto, A. *J. Phys. Chem.* **1995**, *99*, 5058.
(51) Folkesson, B.; Larsson, R. *J. Electron Spectrosc. Relat. Phenom.* **1990**, *50*, 251.
(52) Patil, V.; Oke, S.; Sastry, M. *J. Electron Spectrosc. Relat. Phenom.* **1997**, *85*, 249.
(53) Cerofolini, G. F.; Re, N. *Chem. Phys. Lett.* **2001**, *333*, 181.
(54) Bachrach, S. M. In *Reviews in Computational Chemistry*, Vol 5; Lipkowitz, K. B., Boyd, D. B., Eds.; VCH: New York, 1994; p 171.
(55) Sanderson, R. T. *Science* **1951**, *114*, 670.
(56) Nalewajski, R. F. *J. Am. Chem. Soc.* **1984**, *106*, 944.
(57) Mortier, W. J.; Ghosh, S. K.; Shankar, S. *J. Am. Chem. Soc.* **1986**, *108*, 4315.
(58) Parr, R. G.; Donnelly, R. A.; Levy, M.; Palke, W. E. *J. Chem. Phys.* **1978**, *68*, 3801.
(59) Parr, R. G.; Pearson, R. G. *J. Am. Chem. Soc.* **1983**, *105*, 7512.
(60) Mulliken, R. S. *J. Chem. Phys.* **1934**, *2*, 782.
(61) Lang, N. D.; Kohn, W. *Phys. Rev. B* **1970**, *3*, 1215.
(62) Garcia-Moliner, F.; Flores, F. *Introduction to the Theory of Solid Surfaces*; Cambridge University Press: Cambridge, 1979.
(63) Watanabe, K.; Nakayama, T.; Mottl, J. R. *J. Quant. Spectrosc. Radiat. Transfer* **1961**, *2*, 369.
(64) Crawford, O. H. *Mol. Phys.* **1971**, *20*, 585.
(65) Garrett, W. R. *Chem. Phys. Lett.* **1979**, *62*, 325.

Table 3) and with the results of the DFT calculations on the [AN−M_9] complexes (see Table 1).

However, the chemical potential difference alone does not explain the higher charge transfer observed with nickel and iron as compared to copper, because the metals have similar chemical potentials. This feature can actually be understood from the expression (in the finite-difference approximation) for the charge transferred, ΔN, between two electronic systems A and B:[59]

$$\Delta N = \frac{\mu_A - \mu_B}{\left(\frac{1}{S_A} + \frac{1}{S_B}\right)} \quad (4)$$

This expression is seen to involve not only the chemical potential difference but also the softness S of the isolated reactants: the softer the reactants, the higher the transfer. Because the chemisorption phenomenon is rather local, involving an adsorption site and the adsorbate, it is reasonable to consider, for the metal, the local softness of the adsorption site of the metal surface. This local softness is directly related to the local density of states at the Fermi level.[66] On that basis, we can explain the difference of charge transfer between copper and nickel/iron. The Fermi level of copper is located in the 4s band, where the density of states $g(E_F)$ is much lower than that for nickel/iron, for which E_F is located in the 3d band. This difference in density of states can be directly seen from the UPS spectra of the bare metals displayed in Figure 5. Thus, the local density of states and softness of an adsorption site of the copper surface are expected to be lower than those for a nickel or iron surface. According to eq 4, a smaller charge transfer is expected to occur between Cu and AN than between Ni/Fe and AN.

4.4. Work Function Changes upon Adsorption. 4.4.1. The Case of Chemisorption. The chemisorption of AN on Cu, Ni, and Fe can be used to understand the origin of the work function change upon chemisorption, because the direction of the chemical dipole induced by the partial charge transfer is already known. Work functions are measured from the cutoff of the UPS He(I) spectrum displayed in Figure 5. Because the secondary electron background has a significant contribution of inelastic photoelectrons coming from the metal, the difference between the work function of the AN/metal sample (W_{A-m}) and that of the clean metal (W_m) can be associated with a change in metal work function.

If the chemical dipole potential D_{chem}, because of the partial charge transfer, was the only contribution to the work function change, we should see an increase in work function, because the partial electron transfer occurs from the metal to the AN molecules (vide supra). However, a systematic decrease in work function, $\Delta W = W_{A-m} - W_m = eD_{int} < 0$, is measured upon AN chemisorption: −0.4 eV for Fe, −0.7 eV for Ni, and −0.5 eV for Cu, see Figure 5. This observation implies that the chemical dipole potential must be supersceded by another, more intense dipole potential (that we denote ΔD_{met}), of opposite sign, such that the total interface dipole potential decreases the work function:

$$\Delta W = eD_{int} = eD_{chem} + e\Delta D_{met} \quad (5)$$

Because the negative charge on the chemisorbed AN molecules increases along the series Cu → Ni → Fe (see Table 1), the contribution D_{chem} follows a parallel increase along this series. Although the values of eD_{chem} and $e\Delta D_{met}$ cannot be measured for these systems, the observed decrease in work function indicates an increasingly negative contribution ΔD_{met} along the series Cu → Ni → Fe. It is interesting to note that the increasing contribution of ΔD_{met} along this series follows the increasing value of the (isolated) metal surface dipole potential D_{met} (eD_{Cu} = 3.6 eV, eD_{Ni} = 4.2 eV, eD_{Fe} = 4.9 eV [40]). This suggests that the ΔD_{met} contribution is related to the modification of the metal surface electron density upon adsorption, that is, the change in surface metal dipole upon chemisorption. This is consistent with the fact that the larger the extension of the electron density tail out of the metal, that is, the larger the metal surface dipole potential D_{met}, the more sensitive the electron density tail is to a change in the environment, such as the presence of an adsorbate. This latter effect can be investigated for the case of physisorption, for which ΔD_{met} is the contributor to the work function change.

4.4.2. The Case of Physisorption. It has been shown theoretically that the presence of a physisorbed species leads to a shortening of the electron density tail at the metal surface.[67−69] As a result, the metal surface dipole potential D_{met} is expected to be significantly reduced and the work function decreased by the same amount.[61]

The metal surface dipole change upon physisorption can be illustrated with the archetype system for physisorption: Xe adsorbed on various metal surfaces. Because there is no chemisorption, no chemical dipole, the work function change is expected to be directly related to the change in surface metal dipole potential ΔD_{met} (eq 5). Figure 6 confirms that the work function changes, for one Xe monolayer coverage (as reported by Chen et al.[70]), are related to the metal surface dipole estimated by Lang et al. from jellium model calculations.[40] To a first approximation, a linear relation $\Delta W \cong 0.2 \times eD_{met}$ can be extracted from Figure 6 and can be considered as a characteristic feature of physisorption.

5. Discussion

The data described in the previous section indicate that in every case, that is, whether dealing with a chemisorption or physisorption process, a major contribution to the metal work function change upon adsorption is the shortening of the metal surface electron density tail; this always leads to a decrease of the metal surface dipole potential ΔD_{met}. For a physisorption process, this is the only contribution to the metal work function change: $\Delta W = e\Delta D_{met}$. This is, for instance, the case for inert gases or alkane molecules deposited on nonreactive metal surfaces.[71] Thus, a physisorbed layer is expected to decrease the electron injection barrier. However, this becomes a significant effect only for metals with a large metal surface dipole, which is usually the case of metals with a high work function (Figure 6). The strategy of depositing a physisorbed (mono)layer can, for instance, be applied to improve electron injection in field-effect transistors (FETs), because the source electrode can be a high work function metal. In contrast, for organic-light-emitting diodes (OLEDs), a low work function metal is

(66) Yang, W.; Parr, R. G. *Proc. Natl. Acad. Sci. U.S.A.* **1985**, *82*, 6723.
(67) Lang, N. D. *Phys. Rev. Lett.* **1981**, *46*, 842.
(68) Lang, N. D.; Williams, A. R. *Phys. Rev. B* **1982**, *25*, 2940.
(69) Price, D. L.; Halley, J. W. *Phys. Rev. B* **1988**, *38*, 9357.
(70) Chen, Y. C.; Cunningham, J. E.; Flynn, C. P. *Phys. Rev. B* **1984**, *30*, 7317.
(71) Yoshimura, D.; Ishii, H.; Ouchi, Y.; Ito, E.; Miyamae, T.; Hasegawa, S.; Okudaira, K.; Ueno, N.; Seki, K. *Phys. Rev. B* **1999**, *60*, 9046.

generally required to ensure a low barrier for electron injection; such metals have a small metal surface dipole and are expected to show only a small work function decrease upon physisorption.

For a chemisorption process, the work function change is because of the interface dipole that consists of two contributions (eq 5). As a function of the balance between these two contributions, several cases can appear:

The first case is when partial electron transfer occurs from the adsorbate to the metal, when $\mu_m < \mu_A$ (or in the finite-difference approximation: $W > {}^1/_2(\mathrm{IP} + \mathrm{EA})$). Here, the chemical dipole potential D_{chem} also contributes to a decrease in the metal work function, $\Delta W < 0$. For such adsorbates, both the D_{chem} and the ΔD_{met} dipoles point in the same direction and lead to a strong work function decrease. For instance, it has been observed that sodium atoms evaporated on a Rh(111) surface lead to a work function decrease from 5.4 to 2.5 eV for a 0.2 monolayer coverage,[72] the alkali atoms undergoing a nearly complete charge transfer.[73]

The second case is when the partial electron transfer occurs from the metal to the adsorbate, that is, when $\mu_m > \mu_A$ (or in the finite-difference approximation: $W < {}^1/_2(\mathrm{IP} + \mathrm{EA})$). Two situations are possible:

(i) For a large charge transfer, the chemical dipole potential D_{chem} can be larger than ΔD_{met} in absolute value. Because the two dipoles now point in opposite directions, the resulting interface dipole is characterized by an increase in metal work function, $\Delta W > 0$. This is the only situation leading to a metal work function increase upon monolayer adsorption. Hence, an adsorption characterized by $\Delta W > 0$ has to correspond to a chemisorption process. A well-known example is chlorine adsorbed on metal surfaces; because the Cl atoms undergo almost a complete charge transfer and become anions,[42] a work function increase occurs.[74] For organic molecules, potentially interesting for organic-based electronic devices, work function increases have been reported and associated to a charge transfer from the metal to the molecules; this is the case, for instance, for tetracyanoquinodimethane (TCNQ) on Au,[75] perylene-3,4,9,10-tetracarboxylic-dianhydride (PTCDA) on Mg, In, and Sn,[6] or 3,4,9,10-perylenetetracarboxylic bisimidazole (PTCBI) on Mg.[76] The adsorption of such molecules on the drain electrode in a FET or on the metal anode in a photovoltaic cell is expected to decrease the hole injection barrier and improve device performance. To obtain a high charge transfer, eq 4 indicates that a large chemical potential difference between the metal and the adsorbate is required, as well as a large value of the adsorbate softness and a high density of states at the Fermi level at the adsorption site. Because a large softness is related to a large polarizability of the electronic clouds,[77−80] charge transfer upon chemisorption is expected to be favored for highly polarizable molecules, such as π-conjugated compounds.

(ii) For a small charge transfer, $D_{chem} < \Delta D_{met}$, and the resulting interface dipole leads to a net work function decrease, $\Delta W < 0$. This is the intermediate case found for acrylonitrile chemisorbed on Fe, Ni, and Cu. While the barrier height for charge injection is related to the work function change, the barrier width is expected to depend on the type of interface; a physisorbed layer ($\Delta W < 0$) and a chemisorbed layer with $\Delta W < 0$ are likely to provide different barrier widths for charge injection. For a physisorbed monolayer, its electronic levels do not match the energy levels of the incoming electron and therefore constitute a tunnel barrier between the metal and the active organic material. A chemisorbed layer is expected to participate actively in the charge transfer (injection) process because the surface electron density of the metal is partially delocalized over the chemisorbed molecules[81] and the frontier electronic levels of the chemisorbed molecules are split over a wide energy range.[19]

6. Conclusion

One origin of the interface dipole formed at organic semiconductor/metal interfaces is the charge transfer between the organic layers and the metal upon chemisorption of the organic molecules on the metal surface. The concept of chemical potential equalization described in the framework of density functional theory has been used to rationalize this charge-transfer process. The direction of charge transfer can be estimated from properties of the isolated components (the bare metal and the isolated molecule) that are experimentally accessible: the work function of the bare metal and the ionization potential and electron affinity of the molecule. The prediction of the direction of charge transfer obtained in this way is in good agreement with both the results of an experimental approach using XPS and the results of a theoretical approach where full quantum-mechanical calculations are performed on complexes composed of an adsorbate and a metal surface model.

It appears that the interface dipole, measured as the metal work function change upon adsorption of an organic monolayer, can be divided into two components: (i) the "chemical" dipole, D_{chem}, induced by a partial charge transfer between the adsorbate and the metal upon chemisorption, and (ii) the change in metal surface dipole, ΔD_{met}, because of the modification of the metal surface electron density tail induced by the interaction with the adsorbate. In both cases, the influence of the nature of the metal and the adsorbate can be estimated qualitatively. Therefore, we believe that the results described in this work can provide guidance to tune the interface dipole and, as a result, the barrier for charge injection in organics-based (opto)electronic devices.

Acknowledgment. The Mons−Linköping collaboration is supported by the European Commission "Research and Training Network LAMINATE". The work at Arizona is partly supported by the National Science Foundation (CHE-0071889), the Office of Naval Research, the Petroleum Research Fund, and an IBM Shared University Research program. The work in Mons is partly supported by the Belgian Federal Government "Service des Affaires Scientifiques, Techniques et Culturelle (SSTC)" in the framework of the "Pôle d'Attraction Interuniversitaire en Chimie Supramoléculaire et Catalyze Supramoléculaire" (PAI 4/11) and FNRS-FRFC. X.C. is grant holder of a Marie-Curie Individual Fellowship (contract HPMF-CT-2000-00646). R.L.

(72) Somorjai, G. A. *Introduction to Surface Chemistry and Catalysis*; John Wiley & Sons: New York, 1994.
(73) Lang, N. D. *Phys. Rev. B* **1971**, *4*, 4234.
(74) Anderson, J. R.; Thompson, N. *Surf. Sci.* **1971**, *28*, 84.
(75) Ishii, H.; Sugiyama, K.; Yoshimura, D.; Ito, E.; Ouchi, Y.; Seki, K. *IEEE J. Quantum Electron.* **1998**, *4*, 24.
(76) Hill, I. G.; Schwartz, J.; Kahn, A. *Org. Electron.* **2000**, *1*, 5.
(77) Politzer, P. J. *J. Chem. Phys.* **1987**, *86*, 1072.
(78) Vela, A.; Gazquez, J. L. *J. Am. Chem. Soc.* **1990**, *112*, 1490.
(79) Ghanty, T. K.; Ghosh, S. K. *J. Phys. Chem.* **1993**, *97*, 4951.
(80) Hati, S.; Datta, D. *J. Phys. Chem.* **1995**, *99*, 10742.
(81) Crispin, X.; Geskin, V.; Bureau, C.; Lazzaroni, R.; Schmickler, W.; Brédas, J. L. *J. Chem. Phys.* **2001**, *115*, 10493.

is "Directeur de Recherches du Fonds National de la Recherche Scientifique (FNRS)". J.C. is an FNRS Research Associate.

Appendix

The electrostatic potential energy $\phi(x)$ (in eV)[43] obtained from a jellium model characterized by a Wigner−Seitz radius ratio $r_s/a_0 = 2$ (and therefore $f(x)$) can be fitted with a sigmoid function:

$$e\phi(x) = e\phi_{in} + \frac{eD_{met}}{\left[1 + \exp\left(\frac{-x}{b}\right)\right]^c} \quad \text{and}$$

$$f(x) = 1 - \frac{1}{\left[1 + \exp\left(\frac{-x}{b}\right)\right]^c}$$

with coefficient $b = 0.2978$ and exponent $c = 1.6519$. The $f(x)$ function can be directly extracted from this interpolated function, such that

$$e\phi(x) = e\phi_{in} - eD_{met}\cdot f(x) + eD_{met}\cdot f(x)$$

is zero for an adsorbate physisorbed on the metal surface, that is, typically for a distance x twice larger than the image plane position x_{im} of the metal surface. The value of $f(x)$ is close to unity for an adsorbate on the plane of surface nuclei, that is, at $x = -{}^1/_2 d_{M-M}$ (the zero for the x axis perpendicular to the surface is the position of the jellium edge, that is, one-half the interatomic layer distance ${}^1/_2 d_{M-M}$ from the plane of surface nuclei), see Figure 4. Because Fe, Cu, and Ni have a similar electron density, the b and c parameters characterizing the decay of their electrostatic potential are expected to be similar. Among these metals, the electrostatic potential differs mainly by the value of the inner potential ϕ_{in} and the surface metal dipole potential D_{met}. Thus, we assume that $f(x)$ is similar for Cu, Fe, and Ni. Because the distance between the nuclei of AN and the plane of surface metal nuclei is similar whatever the metal (1.9 Å), the values for $f(x)$ to be considered for chemisorbed AN on Cu(100), Ni(100), and Fe(100) are expected to be similar and equal to $f(x = 1.9\ \text{Å}) = 0.05$.

JA025673R